

Recent Research in Science and Technology 2011, 3(4): 149-154
 ISSN: 2076-5061
www.recent-science.com



PHYSICS

PRECISE EVALUATION OF NEUTRON ASYMMETRY BY THERMODYNAMICAL BAG MODEL

K. Ganesamurthy¹ and S. Kolangi Kannan^{2*}

¹Department of Physics, Urumu Dhanalakshmi College, Trichy-620 019, India

²Department of Physics, J.J College of Engineering & Technology, Trichy-620 009, India

Abstract

Neutron spin asymmetry (A_1^n) and the polarized structure functions (g_1^n, xg_1^n) is precisely evaluated in the kinematic region $0.1 < x < 0.9$ and $Q^2 > 1 \text{ GeV}^2$ by Thermodynamical Bag Model (TBM). The results for A_1^n and g_1^n at $x=0.33$ are consistent with improved precision. The evaluated values of neutron asymmetry are consistent with HERMES data showing a zero crossing around $x=0.47$, and the value at $x=0.60$ is significantly positive. The result agrees with constituent quark model predictions at high x , but disagrees with that from leading-order perturbative QCD (pQCD) assuming helicity conservation.

Keywords: Parton distribution functions, Bag model, Asymmetry

Introduction

The structure functions of the nucleon as measured by deep inelastic scattering (DIS) of leptons from nucleons have, over the last 30 years received much attention. In particular, the evolution with momentum transfer Q^2 has been quantitatively understood in terms of quantum chromodynamics (QCD). The neutron asymmetry measured by HERMES[1,2] and other experiments reveal the understanding of nucleon spin content. During the last decade, the interest has been concentrated on the spin structure functions. Much of this interest was due to the fact that the integral over the experimental spin structure function $g_1(x)$ yielded values that were much lower than the ones expected in the naive quark model [3]. The presence of this "spin crisis" has led to many different ideas on how to account for the nucleon spin. It also has been pointed out early on [4] that the non-relativistic quark model overestimates the quark contribution to the nucleon spin. Relativistic effects lead to a reduction with the gluon contribution is believed to provide the main explanation for the low integral over the spin structure function g_1 . Relativistic effects are expected to play an important role as the masses of quarks are small compared with their momenta. The non-relativistic quark models for instance also overestimate the axial vector weak coupling constants which experimentally amount to $g_A/g_V = 1.26$ rather than $5/3$. Calculations with the MIT bag model [5] or using light-cone quantization [6] have indicated that the lower components of the wave function present in a relativistic description lead to an Opposite contribution to the one of the upper

components, which could generate in the limit of massless quarks, a reduction factor of 0.65 [7].

The spin of the nucleon has its origin in quark, gluon polarizations and in angular momenta. Experimentally, new data on the longitudinal spin structure of the nucleon enable a precise determination of the flavour separated quark polarization distributions in the nucleon. Theoretically, the introduction of generalized parton distributions provides a new unified framework to access dynamic correlations between partons in the nucleon on the basis of various quite different reactions. Originally, it was assumed that the spin of the nucleon (of $1/2$) could be fully attributed to the spin of the quarks. It was assumed that the spin of two quarks cancels and that the remaining quark gives the spin of the nucleon. It was observed that only a small fraction ($14 \pm 9 \pm 21\%$) of the proton spin could be attributed to the quark spins. After the EMC experiment and other experiments carried out at SLAC, CERN and DESY confirmed the small value of $\Delta\Sigma$ reported by EMC.

The spin structure of the nucleon has been investigated in polarized lepton scattering experiments [8-14]. These measurements, most of which covered the deep inelastic scattering (DIS) region of large final-state invariant mass W and momentum transfer Q^2 . The Q^2 -dependence of the polarized structure function g_1 with pQCD evolution equations shed a new light on the structure of the nucleon. The small fraction of the nucleon spin (20%–30%) carried by the quark helicities is in disagreement with quark model expectations of 60%–75%. This reduction is often attributed to the effect of a negatively polarized quark sea at low

* Corresponding Author, Email: skolangikannan@gmail.com

momentum fraction x , which is typically not included in quark models [15]. For a more complete understanding of the quark structure of the nucleon, it is advantageous to concentrate on a kinematic region where the scattering is most likely to occur from a valence quark in the nucleon carrying more than a fraction $x = 1/3$ of the nucleon momentum. In particular, the virtual photon asymmetry is $A_1(x) \approx g_1(x)/F_1(x)$ here F_1 is the usual unpolarized structure function, can be interpreted in terms of the polarization $\Delta u/u$ and $\Delta d/d$ of the valence u and d quarks in the proton in this kinematic region, while the contribution from sea quarks is minimized. This asymmetry also has the advantage of showing only weak Q^2 -dependence [11,16] making a comparison with various theoretical models and predictions. By measuring $A_1(x)$ at large x , one can test different predictions about the limit of $A_1(x)$ as $x \rightarrow 1$. Non-relativistic Constituent Quark Models (CQM) based on SU(6) symmetry predict $A_1(x) = 5/9$ for the proton, $A_1(x) = 0$ for the neutron and $A_1(x) = 1/3$ for the deuteron (modified by a factor $(1 - 1.5\omega_D)$ for the D -state probability ω_D in the deuteron wave function). Quark models that include some mechanism of SU(6) symmetry breaking [15] predict that $A_1(x) \rightarrow 1$ for all three targets as x tends to 1. This is because target remnants with total spin 1 are suppressed relative to those with spin 0. The same limit for $x \rightarrow 1$ is also predicted by pQCD [16], since hadron helicity conservation suppresses the contribution from quarks anti-aligned with the nucleon spin. $A_1(x)$ would be predicted to be more positive at moderately large x because both u and d quarks contribute with positive polarization [17]. The behavior of $A_1(x)$ at large x [18] is connected with the dynamics of resonance production via duality, leading to several predictions for the approach to $A_1(x \rightarrow 1) = 1$ that depend on the mechanism of SU(6) symmetry breaking. The measurements of the asymmetry A_1 at moderate to high x ($x \geq 0.3$) are an indispensable tool to improve our understanding of the valence structure of the nucleon. In spite of large number of data exist on $A_1(x, Q^2)$, most of the high-energy data have very limited statistics at large x and therefore this leads to large uncertainties. Those data show for the first time a positive asymmetry A_1^n at large x , but agree better with predictions [15] that assume negative d -quark polarization $\Delta d/d$ even at large x . In the present work, we have evaluated the polarized structure functions (g_1^n, xg_1^n) and the first high-precision measurement of $A_1(x, Q^2)$ for the neutron at moderate to large x ($x \rightarrow 1$) over a momentum transfer $Q^2 > 1 \text{ GeV}^2$. The results are compared with the world data.

Thermodynamical Bag Model

In TBM, the Fermi and Bose distributions are used to derive the quark and gluon distributions in the infinite momentum frame (IMF). Here the quarks and gluons are treated as fermions and bosons respectively, confined in a volume V at temperature T . The invariant mass W of the excited nucleon is identified with that of the final hadronic system. This is derived from the hypothesis that, the energy transfer to the nucleon causes heating up of the constituent quark gluon system expressed as,

$$(1)$$

Where $\varepsilon_u, \varepsilon_d$, and ε_g are the energy densities of u, d quarks and gluons at a temperature T . The square of the invariant mass is given by,

$$W^2 = M^2 + 2M\nu - Q^2 \quad (2)$$

By solving Eqs (1) and (2) simultaneously by fixing Q^2 , the chemical potentials μ_u and μ_d of u and d quarks are evaluated, which satisfy the number of valence quarks in proton and neutron respectively. The decrease in the value of the Bjorken variable x yields the increase of invariant mass of the final hadronic system and this leads to the enormous production of sea quarks and gluons. At lower values of x , energy transfer is very much greater than the momentum transfer, and this represents the excited state of the target nucleon [19].

The rise in the temperature [20] results in the corresponding increase in the volume of the bag and decrease in the chemical potentials, from which the quark and spin distribution functions are evaluated. The thermal equilibrium of the model is meant for the process involved in the interaction between lepton and nucleon. The quark distribution are deduced from the Fermi function and then transformed to the infinite momentum frame [21].

The quark and gluon distributions are derived from Fermi and Bose distribution functions and these are transferred to the infinite momentum frame which is expressed as [22],

$$u(x) = \frac{6V}{4\pi^2} M^2 T x \ln \left\{ 1 + \exp \left[\left(\frac{1}{T} \right) \left(\mu_u - \left(\frac{Mx}{2} \right) \right) \right] \right\} \quad (3)$$

$$d(x) = \frac{6V}{4\pi^2} M^2 T x \ln \left\{ 1 + \exp \left[\left(\frac{1}{T} \right) \left(\mu_d - \left(\frac{Mx}{2} \right) \right) \right] \right\} \quad (4)$$

The unpolarized structure function of the proton and neutron are given by,

$$F_2^p(x) = x \left\{ \frac{4}{9} [u(x) + \bar{u}(x)] + \frac{1}{9} [d(x) + \bar{d}(x)] \right\} \quad (5)$$

$$F_2^n(x) = x \left\{ \frac{1}{9} [u(x) + \bar{u}(x)] + \frac{4}{9} [d(x) + \bar{d}(x)] \right\} \quad (6)$$

These equations include the contribution of both valence and sea quarks to the nucleon structure function. The spin dependent structure functions

$g_1^p(x)$ and $g_1^n(x)$ are given by,

$$g_1^p(x) = \frac{1}{2} \left[\frac{4}{9} \Delta u(x) + \frac{1}{9} \Delta d(x) + \frac{1}{9} \Delta s(x) \right] \quad (7)$$

$$g_1^n(x) = \frac{1}{2} \left[\frac{1}{9} \Delta u(x) + \frac{4}{9} \Delta d(x) + \frac{1}{9} \Delta s(x) \right] \quad (8)$$

Where $\Delta u(x)$ and $\Delta d(x)$ are the spin distribution function of the u , d with sea quarks given by,

$$\Delta u(x) = \cos 2\theta(x) \left\{ [u(x) + \bar{u}(x)] - \frac{2}{3} [d(x) + \bar{d}(x)] \right\} \quad (9)$$

$$\Delta d(x) = -\cos 2\theta(x) \left\{ \frac{[d(x) + \bar{d}(x)]}{3} \right\} \quad (10)$$

Where,

$$\cos 2\theta = \left[1.0 + \frac{H_0}{\sqrt{x}} (1-x)^2 \right]^{-1} \quad (11)$$

is known as the spin dilution factor [23]. Here H_0 is a free parameter. H_0 is chosen as 0.07 so that the Bjorken sum rule may be satisfied. In parton model, the structure function $F_2(x)$ is expressed as the weighted sum of the quark distribution functions and hence it is reasonable to expect that the quark distribution function observed in DIS should reflect the feature of excitation and subsequent de-excitation to the ground state. Unless this feature is invoked, naive application of Fermi gas model fails to deduce the quark distribution function. But this feature is incorporated in the thermodynamical bag model. This model has correct asymptotic behavior as $x \rightarrow 1$ [24] and it remarkably explains the abundant experimental data of both polarized and unpolarized nucleon structure function and its asymmetries.

Evaluation of Neutron spin Asymmetry

In quark parton model (QPM), the nucleon is viewed as a collection of non-interacting point-like constituents, one of which carries a fraction x of the nucleon's longitudinal momentum and absorbs the virtual photon [25]. The nucleon cross section is then the incoherent sum of the cross sections for elastic scattering from individual charged point-like partons. Therefore the unpolarized and the polarized structure functions F_2 and g_1 can be related to the spin-averaged and spin-dependent quark distributions as [26],

$$F_1(x, Q^2) = \frac{1}{2} \sum_i e_i^2 q_i(x, Q^2) \quad (12)$$

and

$$g_1(x, Q^2) = \frac{1}{2} \sum_i e_i^2 \Delta q_i(x, Q^2) \quad (13)$$

Where $q_i(x, Q^2) = q_i^\uparrow(x, Q^2) + q_i^\downarrow(x, Q^2)$ is the unpolarized parton distribution function (PDF) of the i^{th} quark, defined as the probability that the i^{th} quark inside a nucleon carries a fraction x of the nucleon's momentum, when probed with a resolution determined by Q^2 . The polarized PDF is defined as $\Delta q_i(x, Q^2) = q_i^\uparrow(x, Q^2) - q_i^\downarrow(x, Q^2)$, where $q_i^\uparrow(x, Q^2)$ and $q_i^\downarrow(x, Q^2)$ is the probability to find the spin of the i^{th} quark aligned parallel (anti-parallel) to the nucleon spin.

According to perturbative QCD (pQCD), when the orbital angular momentum is assumed to be zero, the conservation of angular momentum requires that a quark carrying nearly all the momentum of the nucleon (i.e. $x \rightarrow 1$) must have the same helicity as the nucleon. Furthermore, the ratio of the polarized and the unpolarized structure functions g_1 / F_1 , expected to approach unity as $x \rightarrow 1$. In this kinematic region, one can give an absolute prediction for the structure functions based on pQCD, because of both sea and gluon contributions are small in this region, it is relatively the exact region to test the valence quark model and to study the role of valence quarks and their orbital angular momentum contribution to the nucleon spin.

In our present work, the kinematic region has large Bjorken scaling variable x . In this kinematic region, the valence quarks dominate and ratios of structure functions can be evaluated based on our knowledge of the interaction between the quarks. The asymmetry A_1 (the ratio of the polarized and the unpolarized structure functions g_1 / F_1) is expected to approach 1 as $x \rightarrow 1$, in the limit of large Q^2 value. But in all previous data on the neutron asymmetry A_1^n is either negative or consistent with zero. In specific the region $x > 0.3$, both sea-quark and gluon contributions are small, here more focus on valence quarks can be implemented. The Relativistic constituent quark models (RCQM) includes the orbital angular momentum (OAM) and leading order pQCD assuming hadron-helicity conservation (zero OAM) implies various predictions for the proton down-quark polarized distributions in the valence quark region. QCD calculation, describing OAM at the current quark and gluon level, may agree with the RCQM prediction. The connection between these descriptions is of prime importance to the complete description of the nucleon spin using QCD.

The neutron asymmetry A_1^n is related to the polarized and unpolarized structure function g_1 and F_1 through,

$$A_1^n = \frac{g_1^n}{F_1^n} \quad (14)$$

Since g_1 and F_1 follow roughly the same Q^2 evolution in leading order QCD, A_1 is expected to vary quite slowly with Q^2 .

The Hadron Helicity Conservation (HHC) is based on leading order pQCD where the quark OAM is assumed to be zero. Data on the tensor polarization in elastic scattering [27], neutron pion photo production[28] and the proton form factors[29,30] are in disagreement with HHC predictions. The effects beyond leading-order pQCD, such as the quark OAM [31,32,33], might play an important role in processes involving spin flips. Calculations including quark OAM were performed to interpret the proton form factor data [33]. These kinds of calculations may be possible in the future for analyzing A_1^n and other observables in the large x region. The neutron asymmetry A_1^n also includes other predictions from the LSS Next-to-Leading Order (NLO) polarized parton densities[34], the bag model[35], and the chiral soliton model [36], a global NLO QCD analysis of DIS data based on a statistical picture of the nucleon [37].

Results and Discussions

The results of g_1^n , xg_1^n and A_1^n are shown in Figs1, 2 and 3 respectively. For the structure functions g_1^n , xg_1^n our evaluated results has good agreement with HERMES data[1,2] for $x > 0.1$. The value is consistent only in the large x region put a constraint in our understanding that more sea quarks may dominate in the low x regions.

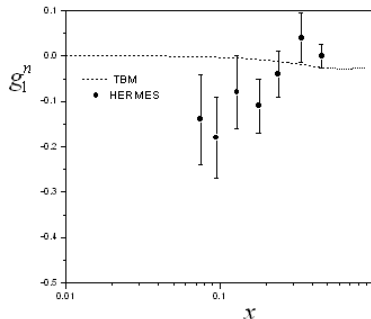


Fig.1: TBM evaluated results on g_1^n at $Q^2 > 1\text{GeV}^2$ is compared with the data from HERMES [1,2]. Error bars in the data includes statistical uncertainties

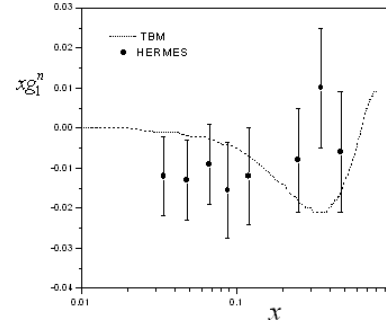


Fig.2: TBM results for xg_1^n vs. x , compared with HERMES[1,2] data of at $Q^2 > 1\text{GeV}^2$. The data represented with statistical errors alone.

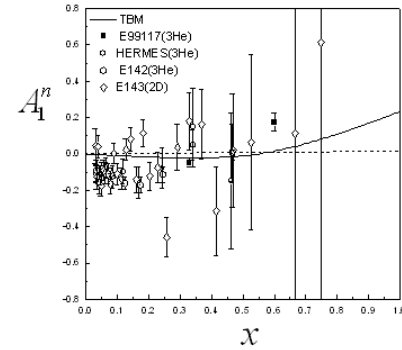


Fig.3: Theoretical evaluated results by TBM for A_1^n are presented for $Q^2 > 1\text{GeV}^2$ compared with HERMES[1,2] and E99117,E142,E143 data. The data includes both statistical and systematic uncertainties

For $x > 0.4$, the results of A_1^n has been improved by about an order of magnitude. It was observed that A_1^n becomes positive at large x . The evaluated values by our model are consistent with the RCQM predictions [15] which suggest that A_1^n becomes increasingly positive at even high x . However they do not agree with LSS(BBS)[38] parametrization in which HHC is imposed. Our results are in good agreement with the LSS 2001 pQCD fit to previous data[34] and a global NLO QCD analysis of DIS data using a statistical picture of the nucleon[37]. The pQCD based HHC suggests that effects beyond leading order pQCD, such as the quark orbital angular momentum may play an important role in this kinematic region. For an evaluation of the Ellis-Jaffe sum rule the integral of g_1^n must be determined at a fixed Q^2 and an extrapolation into the unmeasured x regions must be made. In our work we have applied Bjorken sum rule for the evaluation of the integrals g_1^n and A_1^n . In the present evaluation Q^2 is independent of A_1^n . For a complete understanding of the quark structure of the

nucleon, it is advantageous to concentrate on a kinematic region where the scattering is most likely to occur from a valence quark in the nucleon carrying more than a fraction $x = 1/3$ of the nucleon momentum. By measuring A_1^n at large x , one can test different predictions about the limit of A_1^n as $x \rightarrow 1$. The measurements of the asymmetry A_1^n at moderate to high x ($x \geq 0.3$) are an indispensable tool to improve our understanding of the valence structure of the nucleon.

Conclusions

We have precisely evaluated the spin dependent structure functions of neutron g_1^n, xg_1^n and the asymmetry A_1^n . Our values show a clear picture that A_1^n becomes positive at large x . Our results agree with the LSS 2001 pQCD fit to the previous data and with the RCQM predictions. The values do not agree with the predictions from pQCD based HHC, which suggests that effects beyond leading order pQCD, such as the quark orbital angular momentum may play an important role in this kinematic region. The result evaluated for neutron asymmetry attains positive values as x reaches the maximum range ($x = 1$) is consistent with HERMES data. Recent progress in neutron asymmetry focusing the large x value by Jlab has fed an interesting view in understanding the spin structure of the neutron.

References

1. Akerstaff *et al.*, Phys. Lett. B 404 (1997) 383
2. A. Airapetian *et al.*, Phys. Rev. D 75, 012007 (2007)
3. B. Filippone, X. Ji: The spin structure of the nucleon, Adv. Nucl. Phys. 26, 1 (2001)
4. J.D. Bjorken, Phys. Rev. 148, 1467 (1966)
5. R.L. Jaffe: g_2 : The nucleon's other spin-dependent structure function, Comm. Nucl. Part. Phys. 14, 239 (1990)
6. S.J. Brodsky, F. Schlumpf: Wave function independent relations between the nucleon axial coupling g_A and the nucleon magnetic moments, Phys. Lett. B 329, 111–116 (1994)
7. R.L. Jaffe, A. Manohar: The g_1 problem: fact and fantasy on the spin of the proton, Nucl. Phys. B 337, 509–546 (1990)
8. J. Ashman, *et al.*, EMC Collaboration, Nucl. Phys. B 328 (1989) 1.
9. B. Adeva, *et al.*, SMC Collaboration, Phys. Rev. D 58 (1998) 112001.
10. P.L. Anthony, *et al.*, E142 Collaboration, Phys. Rev. D 54 (1996) 6620, hep-ex/9610007.
11. K. Abe, *et al.*, E143 Collaboration, Phys. Rev. D 58 (1998) 112003, hep-ph/9802357
12. Airapetian, *et al.*, HERMES Collaboration, Phys. Rev. D 71 (2005) 012003, hep-ex/0407032.
13. X. Zheng, *et al.*, Jefferson Lab Hall A Collaboration, Phys. Rev. C 70 (2004) 065207, nucl-ex/0405006.
14. R. Fatemi, *et al.*, CLAS Collaboration, Phys. Rev. Lett. 91 (2003) 222002, nucl-ex/0306019.
15. N. Isgur, Phys. Rev. D 59 (1999) 034013, hep-ph/9809255.
16. P.L. Anthony, *et al.*, E155 Collaboration, Phys. Lett. B 493 (2000) 19, hep-ph/0007248
17. S.J. Brodsky, M. Burkardt, I. Schmidt, Nucl. Phys. B 441 (1995) 197.
18. F.E. Close, W. Melnitchouk, Phys. Rev. C 68 (2003) 035210, hep-ph/0302013.
19. K. Ganesamurthy and R. Sambasivam, Br. J. Phys. 39, 2 (2009).
20. K. Ganesamurthy *et al.*, Mod Phys Lett A, 9 (1994) 3455.
21. F. Takagi, Phys. Rev. D 35 (1987) 2226.
22. K. Ganesamurthy and M. Sathiyamurthy: Ind. J. Phys. A 74 (2000) 53.
23. R. Carlitz, and J. Kaur, Phys. Rev. Lett. 38 (1977) 673.
24. Yunhua Zhang, Lijing Shao, and Bo-Qiang Ma, Phys. Lett. B 671 (2009) 30-35.
25. R.P. Feynman, Phys. Rev. Lett. 23, 1415 (1969).
26. A.W. Thomas and W. Weise, *The structure of Nucleon*, p.78, p.100, p.105-106, Wiley-Vch, Germany (2001)
27. D. Abbott *et al.*, Phys. Rev. Lett. 84, 5053 (2000).
28. K. Wijesooriya *et al.*, Phys. Rev. C 66, 034614 (2002).
29. M.K. Jones *et al.*, Phys. Rev. Lett. 84, 1398 (2000).
30. O. Gayou *et al.*, Phys. Rev. Lett. 88, 092301 (2002).
31. G.A. Miller and M.R. Frank, Phys. Rev. C 65, 065205 (2002);
32. R.V. Buniy, P. Jain and J.P. Ralston, in *AIP Conf. Proc.* 549, 302 (2000).
33. A.V. Belitsky, X. Ji and F. Yuan, arXiv: hep-ph/0212351; X. Ji, J.-P. Ma and F. Yuan, Nucl. Phys. B 652, 383 (2003).
34. E. Leader, A.V. Sidorov and D.B. Stamenov, Eur. Phys. J. C 23, 479 (2002).
35. C. Boros and A.W. Thomas, Phys. Rev. D 60, 074017 (1999).
36. H. Weigel, L. Gamberg and H. Reinhardt, Phys. Lett. B 399, 287 (1997); Phys. Rev. D 55, 6910 (1997).
37. C. Bourrely, J. Soffer and F. Buccella, Eur. Phys. J. C 23, 487 (2002).
38. E. Leader, A.V. Sidorov, D.B. Stamenov, Int. J. Mod. Phys. A 13, 5573 (1998).